GE Healthcare

Nanoparticle diffraction gratings for DNA detection on photopatterned glass substrates

Iuliana E. Sendroiu and Robert M. Corn[a)]
Department of Chemistry, University of California–Irvine, Irvine, California 92697

(Received 23 May 2008; accepted 14 July 2008; published 16 January 2009)

An *ex situ* nanoparticle DNA detection assay utilizing DNA-modified nanoparticles attached to DNA monolayer gratings on glass substrates is developed. The assay utilizes the simultaneous hybridization of a single stranded DNA (ssDNA) target molecule to both an amine-modified DNA oligonucleotide attached to an amine-reactive glass surface and a thiol-modified DNA oligonucleotide attached to a 13 nm gold nanoparticle. Surface plasmon resonance imaging measurements are used to characterize the two sequential hybridization adsorption processes employed in the assay, and fluorescence microscopy is used to characterize the formation of DNA monolayer gratings via the photopatterning of the amine-reactive glass slides. First order diffraction measurements utilizing incoherent collimated white light source and a 10 nm bandpass filter centered at 600 nm provided quantitative measurements of target ssDNA down to a concentration of 10 pM. Fourth order diffraction measurements employing a HeNe laser and avalanche photodiode were used to detect target ssDNA adsorption from 10 μl of a solution with a concentration as low as 10 fM, corresponding to 60 000 target DNA molecules. This simple yet sensitive grating-based nanoparticle DNA detection assay should be directly applicable for genetic screening, mRNA expression assays, and microRNA profiling. © *2008 American Vacuum Society.*
[DOI: 10.1116/1.2994689]

I. INTRODUCTION

In the area of genomic screening and diagnostics, there is a current need for the direct detection of multiple DNA and RNA sequences at femtomolar concentrations for various microarray assays including SNP genotyping,[1–5] mRNA expression,[6] and microRNA profiling.[7–9] PCR amplification methods can be used to detect a specific DNA sequence in a genomic material but typically have problems in uniformly amplifying large sets of DNA sequences simultaneously.[10,11] Both direct fluorescence measurements (sandwich assays, molecular beacons)[12,13] and refractive-index-based methods such as surface plasmon resonance (SPR) have been explored as possible direct detection alternatives to multiplexed PCR.[14–16] For example, SPR imaging (SPRI) has been used to directly detect genomic DNA sequences at femtomolar concentrations via the surface enzymatic manipulation of RNA microarrays with ribonuclease H.[17,18] Additionally, DNA-modified gold nanoparticles have been employed in conjunction with surface enzymatic reactions to detect microRNA with SPRI at femtomolar concentrations.[19]

While *in situ* experiments of DNA hybridization onto microarrays with either SPRI or fluorescence microscopy are very accurate and reproducible, there is a demand for quicker *ex situ* detection methods similar to those routinely used in gene expression arrays. DNA hybridization adsorption followed by drying and *ex situ* detection allows for both the easier handling of samples and the detection of very small numbers of molecules via the reduction in target volume (typically down to microliters). Our goal in the work presented here is to create a simple yet sensitive *ex situ* nanoparticle DNA detection assay that can potentially be used in a microarray format based on the formation of diffraction gratings from patterned DNA monolayers on glass substrates.

Gratings have been used in a variety of methods to monitor bioaffinity adsorption in an *in situ* format.[20–27] For example, researchers have used surface gratings (i) to detect biomolecular adsorption onto patterned gold thin films in a transmission geometry,[26] (ii) to monitor changes in patterned polymer films on gold films in an *in situ* prism format,[20–22,24] and (iii) to quantitatively measure protein adsorption onto patterned bioactive monolayers on glass prisms.[25] We recently have used SPR gratings on patterned gold surfaces in an *in situ* prism-based geometry to detect DNA at femtomolar concentrations.[27] In contrast with these previous efforts, the nanoparticle grating measurements described here are implemented in a simple *ex situ* detection scheme in which the sample is dried prior to detection. This *ex situ* detection methodology is commonly used in mRNA expression measurements.[6]

Specifically, in this study we create a simple grating-based assay that utilizes the simultaneous hybridization of a target single stranded DNA (ssDNA) molecule to both an amine-modified DNA oligonucleotide attached to a photopatterned amine-reactive surface and a thiol-modified DNA oligonucleotide attached to 13 nm gold nanoparticles. This assay is depicted schematically in Fig. 1. The two sequential hybridization adsorption processes are characterized with SPRI measurements, and the formation of DNA monolayer gratings via photopatterning of the amine-reactive glass slides is characterized with fluorescence microscopy. First order dif-

[a)]Electronic mail: rcorn@uci.edu

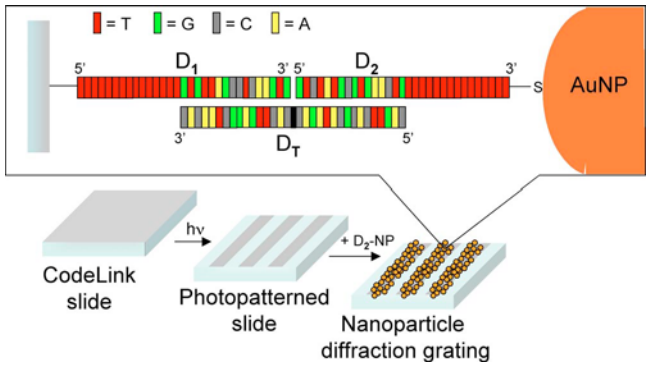

FIG. 1. Schematic illustrating the principle of the nanoparticle-based DNA detection assay on glass substrates. The target ssDNA, D_T, is simultaneously hybridized to a 5′-amine-modified ssDNA (D_1) attached to a photopatterned amine-reactive glass slide and a 3′-thiol-modified ssDNA (D_2) attached to a 13 nm gold nanoparticle. The formation of a nanoparticle grating on the surface is detected by transmission optical diffraction.

fraction measurements obtained with an incoherent collimated white light source are used to detect target ssDNA down to a concentration of 10 pM before background light scattering interferes with the signal. Fourth order diffraction measurements using a HeNe laser and avalanche photodiode allow us to avoid this background and measure target ssDNA adsorption at a concentration of 10 fM in 10 μl of solution. This corresponds to a total amount of 0.1 attomoles or 60 000 target DNA molecules.

II. EXPERIMENTAL CONSIDERATIONS

All chemicals were obtained from commercial sources and used as received. MilliQ water (Millipore) was used throughout.

A. Synthesis of gold nanoparticles capped with ssDNA

Aqueous sodium citrate stabilized Au nanoparticles with a mean diameter of 13 ± 1 nm were synthesized following the Turkevich method.[28] DNA-coated gold nanoparticles were prepared in accordance with well-documented procedures[24,29,30] with the following modification: in the nanoparticle purification stage, removal of excess DNA and reaction by-products was carried out employing $0.2 \times$ SSC at *p*H 7.5 [$1 \times$ SSC=saline-sodium citrate solution, 150 mM NaCl, 15 mM sodium citrate, and 0.1% sodium dodecyl sulfate (SDS)] as diluent. The DNA used was a 3′-thiol-modified single stranded oligonucleotide (D_2, IDT, 5 μl, 1 mM) with the sequence D_2=5′-GTC TAT GCG TGA ACT G$(T)_{15}$-$(CH_2)_3$-SH-3′. The assembly formed of AuNP and D_2 ssDNA is named D_2-NP.

B. Preparation of the glass slides for nanoparticle diffraction gratings

Amine-terminated single stranded DNA (D_1) probes were immobilized at discrete locations onto amine-reactive commercial microarray slides based on *N*-hydroxysuccinimide (NHS) active ester terminated silane (CodeLink) and then hybridized with the target DNA for a sandwich array formation. Amine-reactive microarray glass surfaces were previously studied by Grainger and co-workers[31–33] and their work gives a comprehensive view of the DNA probe immobilization procedure to achieve high target hybridization efficiency.

The first step in preparing DNA sandwich microarrays is the photopatterning, the irradiation of the NHS ester terminated slides with UV light. High energy UV radiation (λ =260 nm, 400 W power from a mercury-xenon arc lamp) was used to irradiate the glass slides through a chromium grating quartz mask (7.5 μm lines) for 1 h. The slides were rinsed with water and dried with nitrogen to remove the NHS-terminated polymer from the exposed areas. Microarrays were fabricated with amine-modified single stranded DNA probes [D_1=5′-NH_2-$(CH_2)_{12}$-$(T)_{15}$ GTG TTA GCC TCA AGT G-3′, IDT Technology)] (200 μM, 10 μl) in 100 mM phosphate buffer, 0.3 M NaCl, and *p*H 8.4. Reactions were run for 24 h using commercial glass coverslips (1 oz., premium cover glass, Fisher Scientific) at room temperature under 100% humidity. All slides were soaked in ethanolamine (50 mM, 0.1*M* tris, *p*H 9, Sigma) at 50 °C for 30 min to block the residual amine-reactive groups followed by incubation in $2 \times$ SSC for 30 min. After all slides were rinsed with water and dried with N_2 gas, the hybridization reaction with a target ssDNA sequence (D_T=5′-CAG TTC ACG CAT AGA CCA CTT GAG GCT AAC AC-3′, IDT Technology) was performed using a range of concentrations from 1 μM to 10 fM and volumes of 10 μl/slide in $2 \times$ SSC under a glass coverslip. The slides were then soaked once in $2 \times$ SSC to remove the coverslip followed by rinsing twice in $0.2 \times$ SSC. The reason for using $2 \times$ SSC as solvent is to optimize the hybridization efficiency on glass, to achieve the ionic strength necessary for the stabilization of backbone interactions in the DNA structure, and to avoid the unspecific binding of the biomolecules or metal particles onto the glass surface, which is assisted by the presence of the SDS surfactant. A second hybridization with a single stranded DNA (D_2) immobilized onto the 13 nm gold nanoparticles surface was then performed on the wet slides. The particles (10 μl, 3.5 nM in $0.2 \times$ SSC) were reacted with the target DNA onto the glass slide for 4 h at room temperature using the glass coverslip. After the hybridization, slides were soaked three times in $0.2 \times$ SSC to remove the coverslip and to make sure all unattached DNA was removed from the glass surface. A schematic of the AuNP diffraction grating formation is shown in Fig. 1, where D_1 and D_2 are each complementary to one-half of the D_T target DNA. For fluorescence imaging experiments, a Cy3 fluorescently labeled (3′ end) single stranded DNA with the same sequence as the D_2 was used (D_2-Cy3). The control experiments were performed under similar conditions as described above with the modification that no target DNA was used in the hybridization reaction. Thus, after the printing step, the photopatterned glass slide possessing the amine ssDNA covalently attached is reacted with the D_2-NP for the diffraction experiments or with D_2-Cy3 for the fluorescence imaging experiments.

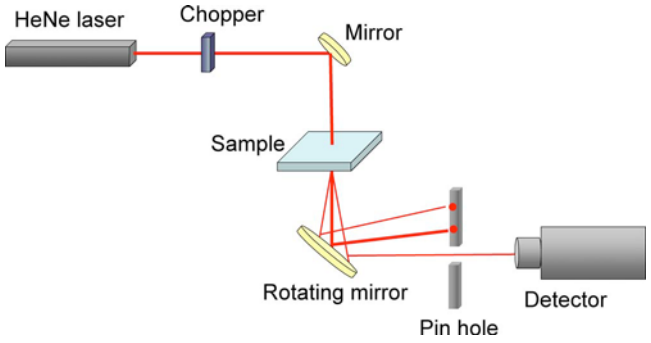

FIG. 2. A simplified representation of the HeNe laser setup used in measuring higher order diffraction spots from DNA-modified nanoparticles attached to DNA monolayer gratings on glass substrates.

C. Preparation of the slides for SPRI experiments

Gold spotted SF10 glass surfaces were reacted with 1 mM ethanolic solution of 11-mercaptoundecylamine (Dojindo) for 24 h. The slides were rinsed with ethanol to remove unbound thiol and dried with nitrogen. The gold spotted slides were then exposed to an aqueous polyglutamic acid (Sigma) solution for 1 h in order to obtain amine-reactive surfaces. The amine DNA, D_1 (10 μl, 0.250 mM) in 0.1M triethanolamine (TEA, Sigma) buffer pH 7.2, was then selectively spotted onto the slide and left to react in the presence of 10 mM 1-Ethyl-3-(3-dimethylaminopropyl) carbodiimide HCl and 10 mM NHS (Pierce) for 48 h in the 100% humidity chamber at room temperature. The role of this was to create reactive succinimide esters on the surface, which can then combine with the amine group of the DNA molecule and form a peptide bond with the available carboxylic acid groups of the polyglutamic acid. The slides were then rinsed with TEA buffer to remove unbound DNA and dried with N_2 gas. Both hybridization reactions with D_T and D_2 ssDNA were performed in the SPR flow cell for 30 min each.

D. Instrumentation

Fluorescence images were taken on an inverted fluorescence microscope (Olympus IX71). Surface plasmon resonance imaging experiments were performed using an SPRimager (GWC Technologies) instrument using protocols that have been described in detail elsewhere.[16,34–36] First order diffraction experiments were performed using a home-built incoherent collimated white light source, made up of a 20 W tungsten lamp and a 10 nm bandpass orange filter centered at 600 nm. The first order diffraction from the sample was measured in transmission mode and focused onto a fiber-optic-coupled monochromator and a charge coupled device (CCD) detector (Ocean Optics). Fourth order diffraction experiments were performed using a laser-based apparatus shown schematically in Fig. 2. This instrument employed a HeNe laser (λ=633 nm, 12 mW, Research Electro-Optics) with the diffracted light measured by a C 5460-01 Hamamatsu avalanche photodiode detector. The glass slide sample was mounted onto a controllable moving stage to enable the laser beam to move over the entire slide.

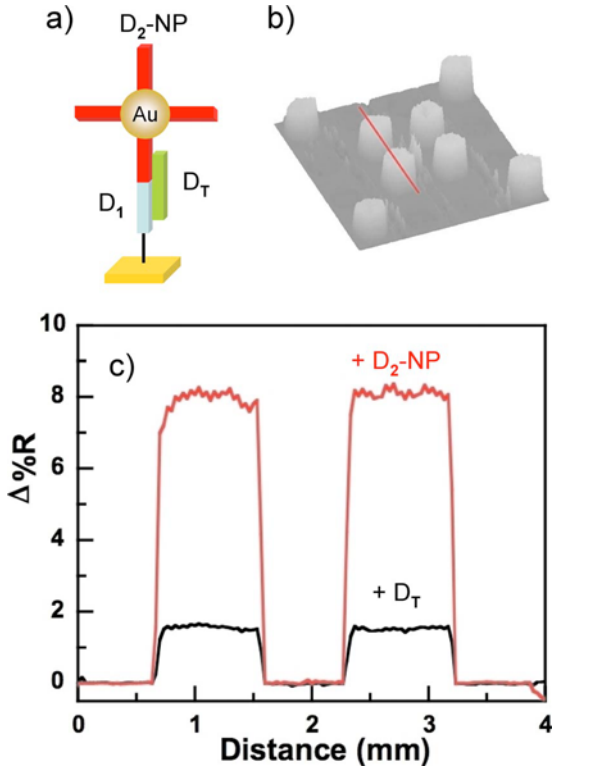

FIG. 3. SPRI data of the nanoparticle-based DNA detection assay on gold substrates. (a) Schematic of the surface assembly after the first (+D_T) and second (+D_2-NP) hybridization adsorption events. (b) SPRI difference image of the hybridization absorption of D_2-NP onto a D_T oligonucleotide array formed by previous hybridization onto a D_1 array. (c) The quantitative line profile of the hybridization of D_1 onto D_T (black line) and of D_2-NP onto D_T (red line) obtained from the array elements indicated by the line in Fig. 2(b).

A rotating mirror was placed behind the sample to give control over the particular diffraction spot that was sent to the detector. An optical chopper (1000 Hz) was used in connection with a lock-in amplifier (SR510, Stanford Research Systems) to measure the ac voltage signal.

III. RESULTS AND DISCUSSION

A. SPRI measurements of the nanoparticle DNA detection assay

A series of SPR imaging measurements on gold thin films was used to verify the presence and activity of the DNA molecules employed in the nanoparticle DNA detection assay. As shown schematically in Figs. 1 and 3(a), this assay requires the assembly of three oligonucleotides on the surface: sequence D_1 that is attached to the planar substrate, sequence D_2 that is attached to the gold nanoparticles, and sequence D_T, the target DNA, which binds to both D_1 and D_2. The three specific DNA sequences used in this study are listed in Sec. II.

SPRI differential reflectivity measurements of a two-component DNA microarray were first used to monitor the "hybridization adsorption" (i.e., DNA duplex formation on the surface) of D_T onto the D_1-modified gold surface. The resultant SPRI image and line profile for the hybridization

adsorption of D_T are shown in Figs. 3(b) and 3(c), respectively. A differential reflectivity change ($\Delta\%R$) of 1.5% was observed upon exposure of the D_1-modified surface to a 1 μM solution of D_T; this $\Delta\%R$ is similar to that observed previously for DNA hybridization adsorption and indicates the formation of a full monolayer of adsorbed D_T.[16,37]

A second SPRI image was obtained after the subsequent exposure of the surface to a 3.5 nM solution of 13 nm gold nanoparticles that were coated with the thiol-modified DNA oligonucleotide D_2. A large differential reflectivity increase (6.5%) was observed due to the adsorption of the gold nanoparticles onto the surface [the red line profile in Fig. 3(c)]. This large increase is attributed to the coupling of the surface and planar plasmon modes in the gold film and the 13 nm particles, as observed previously.[19,38]

From these SPRI measurements, we can conclude that (i) there is a uniform attachment of D_1 oligonucleotides onto the chemically modified gold surface, (ii) the attached D_1 oligonucleotides are able to hybridize with DNA from solution, (iii) the 13 nm gold nanoparticles were successfully modified with thiol-modified D_2 oligonucleotides, (iv) the DNA-modified nanoparticles are capable of hybridization with DNA from solution, and finally (v) the target DNA molecule D_T can simultaneously hybridize to both D_1 and D_2 to form the three-sequence structure shown schematically in Fig. 1. Of course, these SPRI measurements were performed at substantially higher concentrations (high nanomolar) than the intended application range for the diffraction grating measurements (subpicomolar), but they nevertheless confirm that the surface hybridization chemistry required for the nanoparticle-based DNA detection assay is working properly.

B. Monolayer grating fabrication and characterization

A surface grating format was employed to create a simple yet sensitive *ex situ* version of the nanoparticle-based detection assay as described in Fig. 1. In a recent paper,[27] we monitored the nanoparticle-enhanced diffraction from thin film (45 nm) gold gratings with an *in situ* SPR prism geometry to detect ssDNA down to a concentration of 10 fM. In the present study, the nanoparticle DNA detection assay is implemented in an *ex situ* methodology on glass microscope slides. DNA monolayer gratings are created by attaching 5′-amine-modified D_1 DNA onto commercially available amine-reactive silane-coated glass slides (Codelink) that are photopatterned through a Cr mask with UV light. It has been demonstrated previously that organic adsorbed films can be removed completely by exposure to short-wavelength UV radiation by photopatterning.[39,40] Wavelengths shorter than 260 nm are required to photolyze the silane polymer that is then removed from the surface by rinsing with water. The amine-modified ssDNA was then reacted with the surface to create the chemically attached monolayer; any excess amine-reactive sites on the surface were blocked by further reaction of the slides with ethanolamine. In these initial experiments, gratings were formed from evenly spaced 7.5 μm lines; more advanced gratings patterns are envisioned in future experiments.

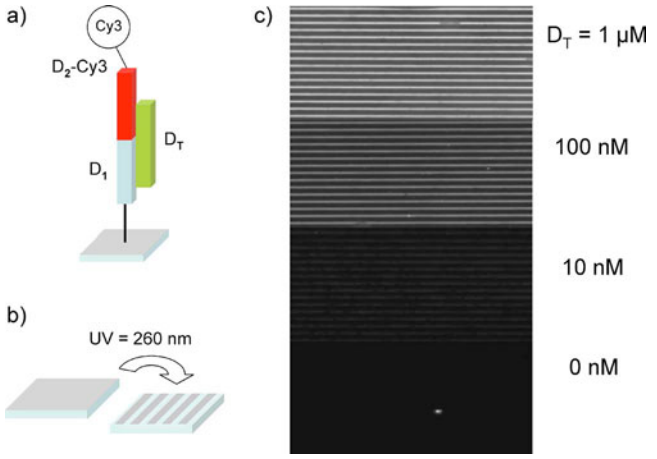

FIG. 4. Fluorescence microscopy data from Cy3-modified DNA monolayers created on photopatterned amine-reactive glass substrates. (a) Schematic of the three-component DNA structure formed on an amine-reactive glass substrate where D_1 is amine-modified ssDNA attached to the surface, D_T is the target oligonucleotide, and D_2-Cy3 is the oligonucleotide D_2 modified with a Cy3 fluorescent tag. (b) An illustration showing the photopatterning of the amine-reactive glass slides by means of a Cr mask with 7.5 μm lines and a high intensity UV radiation source. (c) Fluorescence images of the DNA monolayer gratings after exposure of the slides to target D_T solutions of 1 μM, 100 nM, 10 nM, and 0 nM (as the control slide) followed by a 1 μM D_2-Cy3 solution.

A series of fluorescence microscopy measurements was used to characterize the monolayer grating photopatterning and the DNA surface hybridization adsorption reactions. In lieu of nanoparticles, the D_1-modified grating surface was first exposed to a D_T ssDNA solution, followed by a 1 μM solution of fluorescently labeled D_2 ssDNA (D_2-Cy3). Figure 4 shows representative fluorescence images for D_T solution concentrations of 1 μM to 10 nM. Alternating 7.5 μm dark and light stripes were observed over the entire concentration range, indicating the formation of a DNA monolayer grating on the surface. Also shown in Fig. 4 is a "0 nM" control slide. No patterned fluorescence was observed from this photopatterned slide in spite of its exposure to a 1 μM D_2-Cy3 solution. These experiments allow us to conclude that the amine-reactive surfaces can be photopatterned and then successfully reacted with amine-modified ssDNA to create DNA monolayer gratings and that nonspecific binding of the fluorescent D_2-Cy3 ssDNA is negligible in the nanomolar D_T detection measurements. Detection of D_T using this fluorescence assay was limited to concentrations above 10 pM due to a combination of fluorescence bleaching, CCD sensitivity, and nonspecific fluorescence background.

C. First order diffraction grating experiments with an incoherent light source

Once the specific hybridization adsorption of the DNA-modified nanoparticles and the formation of the DNA monolayer surface grating were thoroughly characterized, the two were combined as shown in Fig. 1 to create the grating-based nanoparticle DNA detection assay. As a first study, we mea-

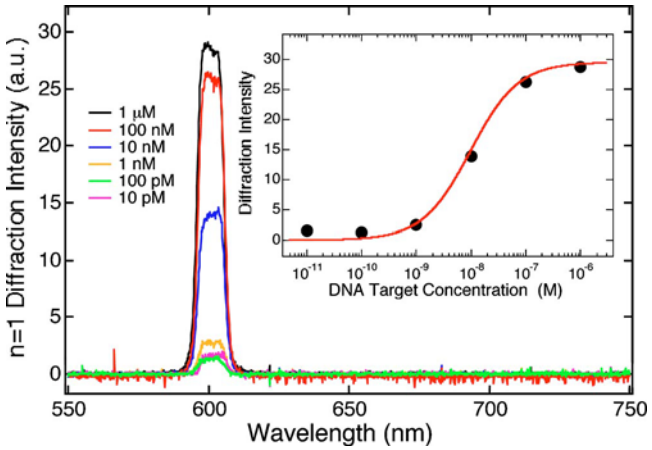

FIG. 5. First order diffraction intensity of the nanoparticle-based DNA detection assay as a function of target D_T concentration. Optical diffraction was obtained using an incoherent light source and a 10 nm bandpass filter centered at 600 nm in transmission; one of the two first order diffraction spots was focused into a fiber-optic-coupled spectrometer to measure the diffraction intensity. The $n=1$ diffraction spectra observed from six different target concentrations are shown in the figure. The inset plots the $n=1$ diffraction intensity at 600 nm vs target DNA concentration on a logarithmic scale. The solid line in the inset is a fit of the data to a Langmuir adsorption isotherm with $K=1.0\times10^8 M^{-1}$.

sured the intensity of the first order diffraction in transmission using a collimated white light source and a 10 nm bandpass filter centered at 600 nm. This wavelength was chosen based on our previous measurements of the diffraction efficiency of 13 nm gold nanoparticles at wavelengths from 400 to 900 nm.[27] The diffraction spot was focused onto a monochromator and quantitated for six target DNA (D_T) concentrations varying from 1 μM to 10 pM. The spectra from the six D_T concentrations are plotted in Fig. 5. In the inset of the figure, the diffraction intensity is plotted versus the log of the D_T concentration and fitted to a Langmuir adsorption isotherm:

$$\Gamma = \Gamma_{\max}\frac{Kc}{1+Kc}, \tag{1}$$

where K is the Langmuir adsorption coefficient, c is the aqueous D_T concentration, Γ is the surface concentration of occupied D_1 surface sites, and $\Gamma_{\max}$ is the total number of D_1 surface sites. The diffraction intensity was assumed to be linearly proportional to $\Gamma/\Gamma_{\max}$, and a Langmuir adsorption coefficient of $1.0\times10^8 M^{-1}$ was obtained from the fit of the data as shown in the inset. This value for K is consistent with the values for the Langmuir adsorption coefficient for DNA hybridization adsorption reported previously.[41]

D. Fourth order diffraction grating experiments with a HeNe laser

For D_T concentrations lower than 10 pM, background scattering of the incident light obscured the first order diffraction in the incoherent light source experiments. This background was avoided and the D_T detection limit was improved to 10 fM by moving to a more powerful light source

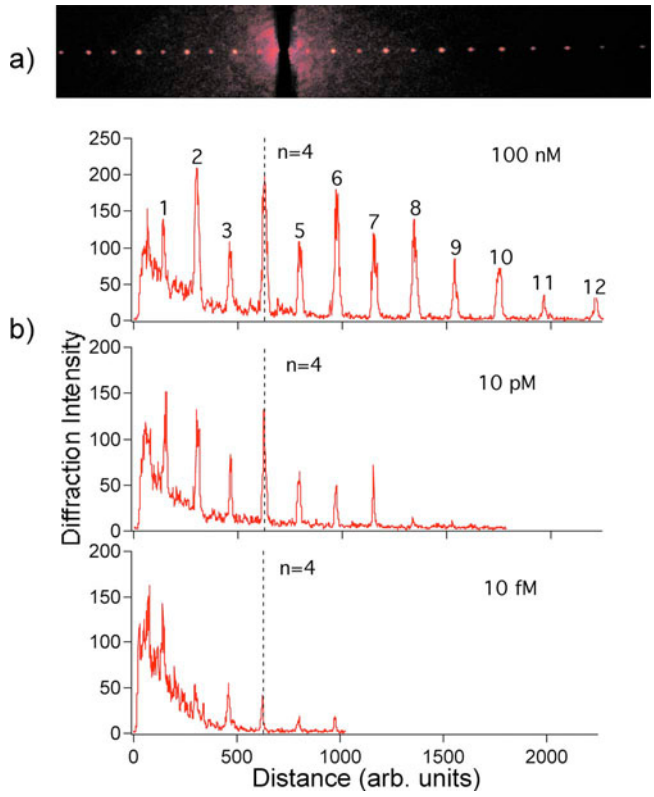

FIG. 6. Laser transmission diffraction pattern images and line profiles from the nanoparticle-based DNA detection assay. (a) Optical image of the diffraction patterned obtained from a nanoparticle grating in transmission using a HeNe laser; for this image, the sample had a target D_T concentration of 100 nM. (b) Line profiles from optical diffraction pattern images obtained from samples with D_T concentrations of 100 nM, 10 pM, and 10 fM, respectively. The $n=4$ diffraction spot is removed from the laser light scattering and speckle background at all three concentrations.

and monitoring higher order diffraction orders. By replacing the white light source with a 12 mW HeNe laser, a multiorder diffraction pattern was observed in transmission. A diffraction image taken from a glass slide that was exposed to a 100 nM D_T solution is shown in Fig. 6(a). As the quantitative line profile in Fig. 6(b) shows, up to 12 diffraction orders were observed. Both the image and the line profile of the 100 nM data show significant speckle and light scattering that appear as a background in the line profile at lower diffraction orders. By choosing an order of $n=4$ or higher, this scattering background can be avoided. An additional even-odd alternation of the diffraction spots was observed for the higher target DNA concentrations where the gratings surface is expected to be significantly occupied with nanoparticles. We attribute this observed alternation to the presence of higher Fourier components in the surface dielectric grating modulation function. A complete calculation of the diffraction efficiency at different wavelengths and multiple orders requires both a rigorous coupled wave analysis[42,43] and calculation of local electromagnetic fields near the gold nanoparticles.[44]

Line profiles from diffraction images obtained at a series of concentrations ranging from 10 pM to 10 fM are shown in Fig. 6(b). The number of higher orders observed in the diffraction pattern decreases as a function of concentration, but

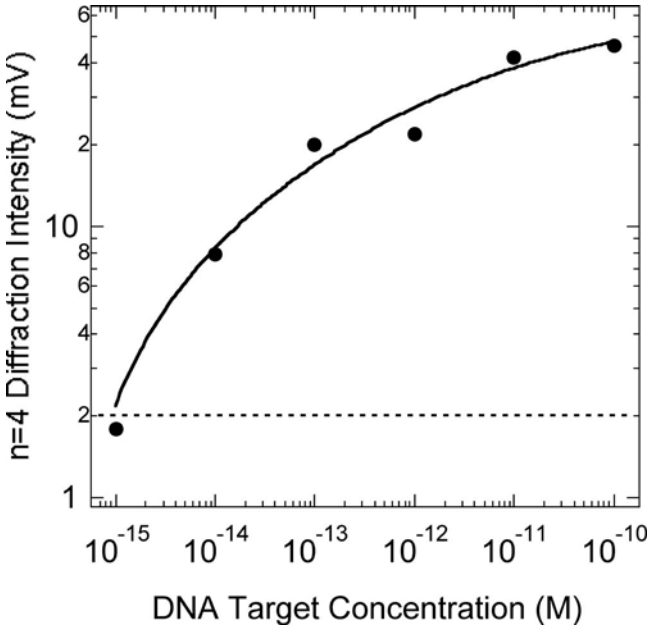

FIG. 7. Fourth order diffraction intensity of the nanoparticle-based DNA detection assay as a function of target D_T concentration. The log of the $n=4$ diffraction intensity as obtained from the avalanche photodiode/lock-in amplifier measurements is plotted vs the log of the target D_T concentration. The dotted line is the background signal level from a control slide that was not exposed to a D_T solution, and the solid line is a parametric fit to the data.

even at 10 fM the $n=4$ diffraction order is clearly visible. The log intensity of the $n=4$ diffraction spot as obtained from the avalanche photodiode/lock-in amplifier measurements is plotted versus the log D_T concentration in Fig. 7. The variation in diffraction spot intensity with concentration is not linear and saturates at concentrations above 1 pM (the solid line is a quadratic fit to the data). This signal saturation is attributed to a combination of nanoparticle surface saturation (one nanoparticle is much larger than a single D_1 adsorption site) and the saturation of the avalanche photodiode used in these experiments. The dotted line in Fig. 7 is the signal level observed from a control slide that was not exposed to a D_T solution; the diffraction intensity from the 1 fM D_T sample is of the same size as this background signal and must be discarded. We thus report the detection limit of these initial surface diffraction measurements of the nanoparticle-based DNA detection assay as 10 fM with a signal to noise ratio of 4. Since a 10 μl D_T solution was used in these *ex situ* measurements, this detection limit corresponds to 60 000 molecules.

IV. CONCLUSIONS

In these initial experiments, we have demonstrated that a simple yet sensitive *ex situ* nanoparticle-based DNA detection assay can be created using the simultaneous hybridization of a target DNA sequence to a DNA monolayer grating and DNA-modified nanoparticles. A detection limit of 10 fM or 60 000 molecules was established using evenly spaced 7.5 μm gratings; further measurements will explore the use of finer gratings, more complex patterns, and, most importantly, the creation of a multiplexed microarray format. We will also explore the use of different nanoparticles (e.g., nanorods) that have potentially larger effects on the grating efficiency at specific wavelengths. Future studies will combine these diffraction measurements with various enzymatic amplification methodologies for even higher sensitivities. As with all *ex situ* DNA hybridization assays, the variability of the hybridization data is higher as compared with *in situ* measurements. However, the intrinsic sensitivity of the diffraction grating format plus its high resistance to nonspecific nanoparticle adsorption strongly suggests that this rapid detection methodology can evolve into a routine technique that can be easily implemented in any laboratory.

ACKNOWLEDGMENTS

This research was supported by the National Institute of Health (Grant Nos. 2RO1 GM059622-04 and 1R21 RR018475-01A2), the National Science Foundation (Grant No. CHE-0551935), and DARPA Micro/Nano Fluidics Fundamentals Focus (MF3) Center at UCI (Grant No. HR0011-06-1-0050). The authors would also like to thank Ara Vehian, Anh Nguyen, and Yulin Chen for their help in optimizing the photopatterning protocols for glass substrates.

[1] A.-C. Syvanen, Nat. Rev. Genet. **2**, 930 (2001).
[2] B. W. Kirk, M. Feinsod, R. Favis, R. M. Kliman, and F. Barany, Nucleic Acids Res. **30**, 3295 (2002).
[3] Y. P. Bao, M. M. Huber, T. Wei, S. S. Marla, J. J. Storhoff, and U. R. Muller, Nucleic Acids Res. **33**, el5 (2005).
[4] D. Gerion, F. Chen, B. Kannan, A. Fu, W. J. Parak, D. J. Chen, A. Majumdar, and A. P. Alivisatos, Anal. Chem. **75**, 4766 (2003).
[5] Y. Li, A. W. Wark, H. J. Lee, and R. M. Corn, Anal. Chem. **78**, 3158 (2006).
[6] M. Schena, D. Shalon, R. Davis, and P. Brown, Science **270**, 467 (1995).
[7] C. Arenz, Angew. Chem. **118**, 5170 (2006); Angew. Chem., Int. Ed. **45**, 5048 (2006).
[8] R. W. Carthew, Curr. Opin. Genet. Dev. **16**, 203 (2006).
[9] A. Rodriguez *et al.*, Science **316**, 608 (2007).
[10] S. F. Gonzalez, M. J. Krug, M. E. Nielsen, Y. Santos, and D. R. J. Call, J. Clin. Microbiol. **42**, 1414 (2004).
[11] S. Sengupta, K. Onodera, A. Lai, and U. J. Melcher, J. Clin. Microbiol. **41**, 4542 (2003).
[12] L. A. Neely *et al.*, Nat. Methods **3**, 41 (2006).
[13] J. S. Hartig, I. Grune, S. H. Najafi-Shoushtari, and M. Famulok, J. Am. Chem. Soc. **126**, 722 (2004).
[14] H. J. Lee, A. W. Wark, and R. M. Corn, Langmuir **22**, 5241 (2006).
[15] H. J. Lee, Y. Li, A. W. Wark, and R. M. Corn, Anal. Chem. **77**, 5096 (2005).
[16] A. W. Wark, H. J. Lee, and R. M. Corn, Anal. Chem. **77**, 3904 (2005).
[17] T. T. Goodrich, H. J. Lee, and R. M. Corn, Anal. Chem. **76**, 6173 (2004).
[18] T. T. Goodrich, H. J. Lee, and R. M. Corn, J. Am. Chem. Soc. **126**, 4086 (2004).
[19] S. Fang, H. J. Lee, A. W. Wark, and R. M. Corn, J. Am. Chem. Soc. **128**, 14044 (2006).
[20] F. Yu, D. Yao, and W. Knoll, Nucleic Acids Res. **32**, e75 (2004).
[21] F. Yu, S. Tian, D. Yao, and W. Knoll, Anal. Chem. **76**, 3530 (2004).
[22] F. Yu and W. Knoll, Anal. Chem. **76**, 1971 (2004).
[23] A. M. Massary, K. J. Stevenson, and J. T. Hupp, J. Electroanal. Chem. **500**, 185 (2001).
[24] S. Tian, N. R. Armstrong, and W. Knoll, Langmuir **21**, 4656 (2005).
[25] J. B. Goh, P. L. Tam, R. W. Loo, and M. C. Goh, Anal. Biochem. **313**, 262 (2003).
[26] R. C. Bailey, J.-M. Nam, C. A. Mirkin, and J. T. Hupp, J. Am. Chem. Soc. **125**, 13541 (2003).
[27] A. W. Wark, H. J. Lee, A. J. Qavi, and R. M. Corn, Anal. Chem. **79**, 6697 (2007).

[28]J. Turkevich, P. C. Stevenson, and J. Hillier, Discuss. Faraday Soc. **11**, 55 (1951).
[29]R. Elghanian, J. J. Storhoff, R. C. Mucic, R. L. Letsinger, and C. A. Mirkin, Science **277**, 1078 (1997).
[30]G. P. Goodrich, M. R. Helfrich, J. J. Overberg, and C. D. Keating, Langmuir **20**, 10246 (2004).
[31]P. Gong and D. W. Grainger, Surf. Sci. **570**, 67 (2004).
[32]F. Cheng, L. J. Gamble, D. W. Grainger, and D. G. Castner, Anal. Chem. **79**, 8781 (2007).
[33]P. Gong, G. M. Harbers, and D. W. Grainger, Anal. Chem. **78**, 2342 (2006).
[34]E. A. Smith and R. M. Corn, Appl. Spectrosc. **57**, 320A (2003).
[35]T. Wilkop, Z. Wang, and Q. Cheng, Langmuir **20**, 11141 (2004).
[36]J. S. Shumaker-Parry and C. T. Campbell, Anal. Chem. **76**, 907 (2004).
[37]B. P. Nelson, T. E. Grimsrud, M. R. Liles, R. M. Goodman, and R. M. Corn, Anal. Chem. **73**, 1 (2001).
[38]L. He, M. D. Musick, S. R. Nicewarner, F. G. Salinas, S. J. Benkovic, M. J. Natan, and C. D. Keating, J. Am. Chem. Soc. **122**, 9071 (2000).
[39]M. C. Howland, A. R. Sapuri-Butti, S. S. Dixit, A. M. Dattelbaum, A. P. Shreve, and A. N. Parikh, J. Am. Chem. Soc. **127**, 6752 (2005).
[40]M. Nakagawa, N. Nawa, and T. Iyoda, Langmuir **20**, 9844 (2004).
[41]A. W. Wark, H. J. Lee, and R. M. Corn, in *Handbook of Surface Plasmon Resonance*, edited by R. B. M. Schasfoort and A. J. Tudos (RSC, Cambridge, UK, 2008), pp. 251–280.
[42]M. G. Moharam and T. K. Gaylord, J. Opt. Soc. Am. **71**, 811 (1981).
[43]M. G. Moharam and T. K. Gaylord, J. Opt. Soc. Am. A **3**, 1780 (1986).
[44]K. L. Kelly, E. Coronado, L. L. Zhao, and G. C. Schatz, J. Phys. Chem. B **107**, 668 (2003).